

Exploiting random phenomena in magnetic materials for data security, logics, and neuromorphic computing: Challenges and prospects


Cite as: APL Mater. 9, 070903 (2021); <https://doi.org/10.1063/5.0055400>

Submitted: 28 April 2021 • Accepted: 10 June 2021 • Published Online: 08 July 2021

 C. Navau and  J. Sort

COLLECTIONS

 This paper was selected as Featured

 This paper was selected as Scilight



View Online



Export Citation



CrossMark

ARTICLES YOU MAY BE INTERESTED IN

[Neuromorphic computing with antiferromagnetic spintronics](#)

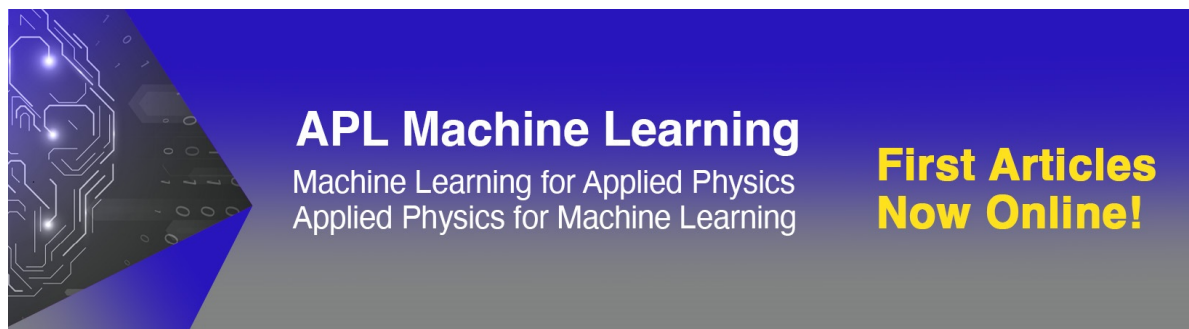
Journal of Applied Physics **128**, 010902 (2020); <https://doi.org/10.1063/5.0009482>

[The design and verification of MuMax3](#)

AIP Advances **4**, 107133 (2014); <https://doi.org/10.1063/1.4899186>

[Advances in magneto-ionic materials and perspectives for their application](#)

APL Materials **9**, 030903 (2021); <https://doi.org/10.1063/5.0042544>



APL Machine Learning

Machine Learning for Applied Physics
Applied Physics for Machine Learning

**First Articles
Now Online!**

Exploiting random phenomena in magnetic materials for data security, logics, and neuromorphic computing: Challenges and prospects



Cite as: APL Mater. 9, 070903 (2021); doi: 10.1063/5.0055400

Submitted: 28 April 2021 • Accepted: 10 June 2021 •

Published Online: 8 July 2021



C. Navau^{1,a)} and J. Sort^{1,2,a)}

AFFILIATIONS

¹ Departament de Física, Universitat Autònoma de Barcelona, E-08193 Cerdanyola Del Vallès, Spain

² Institució Catalana de Recerca i Estudis Avançats (ICREA), Pg. Lluís Companys 23, E-08010 Barcelona, Spain

^{a)} Authors to whom correspondence should be addressed: Carles.Navau@uab.cat and jordi.sort@uab.cat

ABSTRACT

Random phenomena are ubiquitous in magnetism. They include, for example: the random orientation of magnetization in an assembly of non-interacting isotropic magnets; arbitrary maze domain patterns in magnetic multilayers with out-of-plane anisotropy, random polarization, and chirality of an array of magnetic vortices; or Brownian skyrmion motion, among others. Usually, for memory applications, randomness needs to be avoided to reduce noise and enhance stability and endurance. However, these uncontrolled magnetic effects, especially when incorporated in magnetic random-access memories, offer a wide range of new opportunities in, e.g., stochastic computing, the generation of true random numbers, or physical unclonable functions for data security. Partial control of randomness leads to tunable probabilistic bits, which are of interest for neuromorphic computing and for new logic paradigms, as a first step toward quantum computing. In this Perspective, we present and analyze typical materials that exhibit stochastic magnetic phenomena and we show some examples of emerging applications. The current challenges in terms of material development, as well as new strategies to tune stochasticity, enhance energy efficiency, and improve operation speeds are discussed, aiming to provide new prospects and opportunities in this compelling research field.

© 2021 Author(s). All article content, except where otherwise noted, is licensed under a Creative Commons Attribution (CC BY) license (<http://creativecommons.org/licenses/by/4.0/>). <https://doi.org/10.1063/5.0055400>

I. INTRODUCTION

Magnetic materials exhibit a plethora of stochastic (or random) effects. Such randomness occurs in the magnetic orientation of small magnetic nanoparticles over time,¹ in the Brownian trajectories of skyrmion quasiparticles,² or in the polarity and chirality of magnetic vortices generated in micrometer-sized soft-magnetic disks,³ among others. For some applications (e.g., conventional memory devices), randomness is highly undesirable (since it can generate noise and loss of information), and strategies have been put forward to avoid it. However, randomness can be used to generate true random numbers at hardware level or in new computing paradigms,⁴ as will be described in this Perspective. Partial control of randomness with external stimuli (voltage, current, particle/dot shape modifications,

and structural defects) can find applications in logics and in neuromorphic computing. Probabilistic bits (i.e., bits with a probability to occur higher or lower than fully random 50%) are considered a first step toward quantum q-bits.⁵ Figure 1 illustrates the main concepts related to stochasticity in magnetic phenomena and the prospective applications. The goal of this Perspective is to analyze the state of the art of materials and phenomena related to magnetic randomness, with emphasis on the current challenges (control of randomness, energy efficiency, CMOS integration, or operation speed) and future opportunities in different technological fields, encompassing data security, probabilistic computing, or neuromorphic computing (see Fig. 1). The reported effects can be of interest to deal with data in which uncertainty is inherently present. It has been long recognized that probabilistic algorithms can tackle some specific problems

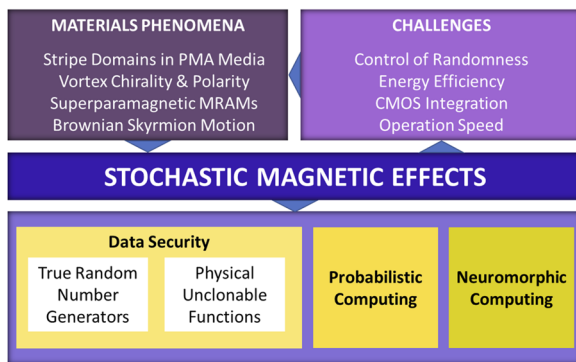


FIG. 1. Illustration of the main phenomena that lead to magnetic random effects and the prospective applications in different research domains. PMA stands for "perpendicular magnetic anisotropy."

much more efficiently than classical algorithms using a deterministic computer.⁶ While the areal density of information in magnetic storage media has been drastically increasing over the years, new challenges posed by artificial intelligence and the need to tackle big data require changes in the computing paradigms, in which stochasticity can play a key role.

II. STOCHASTIC EFFECTS IN MAGNETIC MATERIALS

It is well known that the magnetic dipoles of an assembly of small magnets will orient at random in the as-prepared state or when cooled through the Curie temperature if they are not affected by dipolar interactions. As an example, Fig. 2(b) shows the magnetic-force microscopy (MFM) image of random "up" (white) and "down" (black) single-domain states of an array of Ni pillars with out-of-plane magnetization grown by electrodeposition.⁷

A single-domain nanomagnet can be characterized by an energy barrier (ΔE) that separates two possible states, each of them with the magnetic moment oriented in opposite directions. When the magnet is placed in one of these two states, it stays there for a certain amount time, called "retention time" (τ), which is given by $\tau = \tau_0 \exp(\Delta E/k_B T)$, where τ_0 is a material constant, k_B is the Boltzmann constant, and T is temperature. In a first approximation,

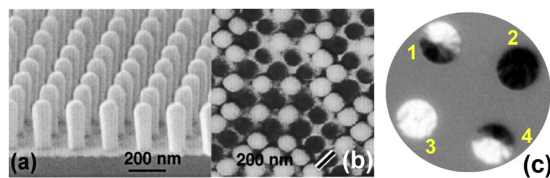


FIG. 2. (a) Scanning electron microscopy (SEM) image and (b) magnetic-force microscopy (MFM) micrographs of an array of Ni pillars (90 nm diameter, 220 nm height), showing random "single-domain" behavior with out-of-plane magnetization. Reproduced from Ross *et al.*, J. Appl. Phys. **91**, 6848 (2002) with the permission of AIP Publishing. (c) Magnetic contrast image acquired by x-ray photoemission electron microscopy (XPEEM) at the Fe L -edge of an array of $\text{Ni}_{80}\text{Fe}_{20}/\text{Ir}_{20}\text{Mn}_{80}$ disks (showing dissimilar magnetic configurations) in the framework of an exchange bias investigation. Reproduced from Salazar-Alvarez *et al.*, Appl. Phys. Lett. **95**, 012510 (2009) with the permission of AIP Publishing.

the energy barrier can be expressed as $\Delta E = \frac{1}{2} M_S V H_K$, where M_S is the saturation magnetization, V is volume, and H_K is the effective anisotropy field. While τ is of the order of years in non-volatile memories, the time can be engineered to be much shorter (sub-second) using suitable nanomaterials (with low H_K , M_S , and V values). When the size of a magnet is sufficiently small (approaching the superparamagnetic limit), its orientation will spontaneously fluctuate with time between two binary states due to thermal agitation. The readout from such tiny magnets, once the magnetic signal is transduced into a voltage or current, will result in telegraphic noise,¹ and this can be considered as a simplified version of a stochastic device. This concept has been applied to magnetic tunnel junctions (MTJs) comprising a free layer with small in-plane magnetic anisotropy (superparamagnetic MTJs), where thermal activation effects induce stochastic fluctuations in the magnetoresistance values at time scales below 5 ns.⁸

In magnetic objects of larger dimensions, the magnetization reversal mode can be tailored to arbitrarily fluctuate between different mechanisms. In a previous work, we adjusted the thickness and diameter of circular magnetic disks to critical values close to the boundaries between single-domain and vortex states so that the disks could reverse their magnetization arbitrarily either by coherent rotation or through vortex formation. This is illustrated in Fig. 2(c), which shows the element-specific polarized x-ray photoemission electron microscopy (XPEEM) image at the Fe L -edge, in the absence of magnetic field applied, of an array of $\text{Ni}_{80}\text{Fe}_{20}$ (6 nm)/ $\text{Ir}_{20}\text{Mn}_{80}$ (5 nm) disks (2 μm in diameter) deposited onto a naturally oxidized Si wafer. Disks 1 and 4 form vortex states at remanence, while disks 2 and 3 are single domains.⁹

Remarkably, even when all disks in an array form vortex states (e.g., in 100 nm-thick $\text{Ni}_{80}\text{Fe}_{20}$ disks with 1 μm diameter), the chirality of the vortex and polarity of the vortex core are random if no symmetry-breaking geometrical constraints are applied to the disk shape (see Fig. 3). The white and black spots at the center of the disks, imaged using full-field magnetic transmission soft x-ray microscopy (MTXM) [see Fig. 3(b)], reveal positive and negative polarity of the vortex core, respectively.³ The chirality is determined from the in-plane magnetic component [Fig. 3(a)], taking into account the vortex core polarity. Another example is continuous multilayers with perpendicular effective anisotropy, which exhibit magnetic domains that form random maze patterns each time the system is demagnetized, provided that there are no structural defects (e.g., grain boundaries) that influence the labyrinthic paths.

There are many other examples of random phenomena in magnetic materials. Steels and other types of ferromagnets exhibit the Barkhausen effect, which is related to noise in the magnetic output signal when the material is subject to an applied magnetic field and the size of the domains fluctuates with time in discrete steps due to structural defects in the crystal lattice.¹⁰ Concerning magnetic "moving entities," stochastic domain wall pinning has been predicted¹¹ in magnetic nanowire devices due to the influence of thermal perturbations on the domain walls' dynamics. Random thermally driven effects also manifest in the trajectories of magnetic skyrmions in unconstrained, defect-free, ultra-thin magnetic films (see Fig. 4).^{12,13} Skyrmions are spin swirling quasiparticles that have generated great expectations in recent years due to their potential to act as small information carriers.¹⁴

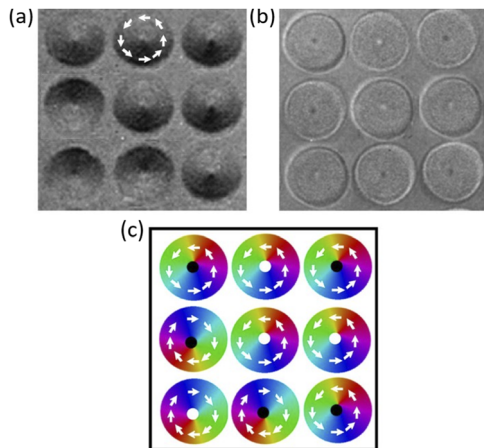


FIG. 3. Full-field magnetic transmission soft x-ray microscopy (MTXM) images of the in-plane (a) and out-of-plane (b) magnetic components taken at remanence in an array of 100-nm-thick $\text{Ni}_{80}\text{Fe}_{20}$ disks ($1\ \mu\text{m}$ diameter). The sense of rotation of the in-plane magnetization (i.e., vortex chirality) is indicated with the white arrows in (a). The black and white spots at the center of the disks are upward and downward vortex cores (positive and negative polarity), respectively (b). The vortex configuration of each disk is illustrated in (c). Reproduced with permission from Im *et al.*, Nat. Commun. **3**, 983 (2012). Copyright 2012, Nature Publishing Group.

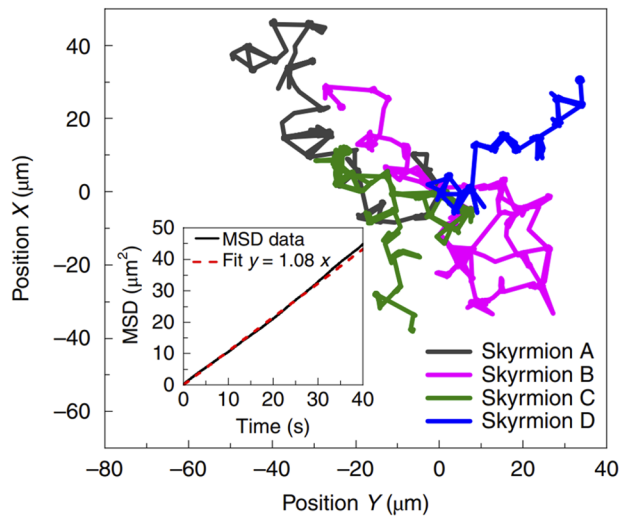


FIG. 4. Non-deterministic trajectories, determined by Kerr microscopy imaging, of selected skyrmions formed at 296 K in Ta (5 nm)/ $\text{Co}_{20}\text{Fe}_{60}\text{B}_{20}$ (1 nm)/Ta (0.08 nm)/MgO (2 nm)/Ta (5 nm) stacks. All the skyrmions were set to start at position (0, 0). The timescale of the observation was in the range of seconds to minutes. The inset shows the time-averaged mean squared displacement (MSD) (black line) and the linear fit of the data (red dashed line). Reproduced with permission from Zázvorka *et al.*, Nat. Nanotechnol. **14**, 658 (2019) Copyright 2019, Nature Publishing Group.

III. IS IT POSSIBLE TO CONTROL RANDOMNESS IN MAGNETIC MATERIALS?

While fully random magnetic effects are appealing for stochastic computing or true random number generators (RNGs) (see Sec. IV), partial control of randomness can yield other interesting

applications. For example, the retention time in low energy barrier nanomagnets, τ , can be manipulated with current or voltage. By doing so, one can generate probabilistic p-bits, which have a probability of being “1” or “0” different than 50% (which would be the fully stochastic case). These p-bits are considered as an intermediate between classical bits (with deterministic “0” and “1” orientations) and quantum q-bits (with coherent superpositions of “0” and “1”).¹

Another example is the control of double-shifted loops in $[\text{Pt}/\text{Co}]_n$ multilayers with out-of-plane magnetization that we could achieve using the coupling with an adjacent antiferromagnetic (AFM) $\text{Ir}_{20}\text{Mn}_{80}$ layer (exchange bias effect).¹⁵ This is illustrated in Fig. 5. Configuration (a) is the typical maze domain patterns with random shapes obtained after demagnetizing the $[\text{Pt}/\text{Co}]_n$ multilayer. An equal proportion of white and dark stripes (indicating regions with “up” and “down” magnetization, respectively) is observed by MFM. When this pattern is coupled to the adjacent AFM layer, a double-shifted loop (50% shifted to the right and 50% shifted to the left) is obtained. By annealing the system close to the exchange bias blocking temperature and subsequently cooling under different magnetic fields, the degree of randomness is decreased. For larger magnetic fields, the amount of “white” regions progressively increases [configuration (b)] while the magnetization amplitude of the left-shifted hysteresis loop also increases. If the system is cooled with a sufficiently high magnetic field, an almost deterministic single-domain state is generated [configuration (c)] and the loop shape approaches that of a single-shifted hysteresis loop.

During the last few years, we have also proposed strategies to manipulate and control the chirality and polarity of magnetic vortices by incorporating asymmetrical variations in the thickness of

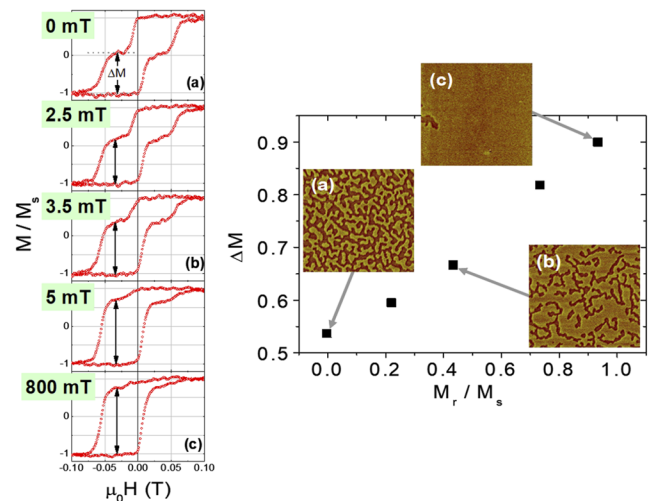


FIG. 5. (Left) Magnetic hysteresis loops measured along the perpendicular to the plane of a $[\text{Pt}/\text{Co}]_n$ multilayer coupled to IrMn, after field cooling from $T = 520\ \text{K}$ using different magnetic field values (H_{FC}). The various loops show the progressive tuning of the vertical magnetization amplitude depending on H_{FC} . (Right) Dependence of the normalized magnetization amplitude of the sub-loop shifted toward the negative fields, ΔM , vs the squareness ratio (M_r/M_s). The insets show the corresponding magnetic-force microscopy images for (a) $M_r/M_s = 0$, (b) $M_r/M_s = 0.43$, and (c) $M_r/M_s = 0.93$. Note that each image has a side length of $20\ \mu\text{m}$. Reproduced with permission from Brück *et al.*, Adv. Mater. **17**, 2978 (2005). Copyright 2005, Wiley.

the dots.¹⁶ A similar approach consists in breaking the circular rotational symmetry by, e.g., asymmetrical notches.¹⁷ Although experimental realization of these effects requires the use of advanced lithographic procedures, these procedures are now quite manageable, and therefore, a variety of works demonstrating geometrical control of the vortex state have been reported.^{18–22}

Very recently, we have also used micromagnetic simulations to study the dynamics of skyrmions in the presence of defects (pinning sites) or borders. The probability that a skyrmion becomes trapped in a pinning center or the probability of its survival along a race-track can be calculated as a function of temperature and the length of the track.²³ Indeed, inherent or artificially created defects in the crystallographic structure of the films can modify the trajectory of skyrmions in a partly deterministic manner.

In spite of the previous examples, a number of different challenges, in terms of materials properties and technological advances, need to be overcome for a successful accomplishment of fully stochastic magnetic effects and the probabilistic (i.e., partial) control of this randomness. Namely, superparamagnetic MTJs require the use of very thin amorphous soft-magnetic layers with very low anisotropy. So far, almost all examples are based on CoFeB. Conversely, for the coupling between FM and AFM domains, a relatively high uniaxial magnetic anisotropy is required in the ferromagnet, while the anisotropy in the antiferromagnet and the size of AFM domains should be small or at least commensurate to the domain size in the ferromagnet. This needs to be accompanied with a relatively high interfacial exchange constant so that the strength of the coupling is sufficient to overcome the magnetostatic energy in the ferromagnet. Finally, formation of skyrmions at room temperature only occurs in a limited number of systems, such as Ta/Co₄₀Fe₄₀B₂₀/TaO_x,^{24,25} in asymmetric Co nanodot arrays with the in-plane magnetic easy axis grown on Co/Pd underlayers with perpendicular anisotropy,²² or in Pt/Co/Ta and Pt/CoFeB/MgO stacks with ultrathin Co and CoFeB layers,²⁶ among others.²⁷ The control of structural defects (e.g., periodic pinning sites) in these layers, with the aim of guiding skyrmions motion, again requires dedicated lithography procedures and is not always straightforward.

IV. HIGHLIGHTS OF EMERGING APPLICATIONS BASED ON MAGNETIC STOCHASTIC EFFECTS

A. Exploiting magnetic randomness for true random number generators

Random numbers play a crucial role in the encryption of secure data for communication and storage purposes. Taxonomically, random number generators (RNGs) can be classified into two large categories: pseudo-RNGs, which use deterministic software algorithms to generate a sequence of random numbers (and are thus vulnerable to hacking cyberattacks), and true-RNGs, which are implemented at the hardware level and generate sequences of random numbers using non-deterministic, uncontrollable physical events (thus being cryptographically more secure).⁴ From a physical viewpoint, true-RNGs can benefit from two types of randomness sources: fluctuations (e.g., thermal noise, shot current noise, and chaotic fluctuation of a semiconductor laser) and stochastic switching events (radioactive decay intervals, magnetization switching in nanomagnets, switching events in resistive-random-access memories (RAMs), and current-triggered random transitions in spintronic spin-transfer-torque

STT-magnetoresistive random-access memories (MRAMs)).^{28,29} In the following, the basic idea of STT-MRAM, in which a pulse generator utilizes the stochastic nature of spin-torque switching in an MTJ to generate true random numbers,²⁸ is illustrated (Fig. 6).

An MTJ consists of two nanoscale ferromagnetic (FM) layers separated by a spacer layer (typically MgO). While the magnetization of one of the layers (“reference” layer) is pinned in a particular direction (usually through the coupling with an antiferromagnet), the magnetization of the other layer (free layer) can be switched by external stimuli, such as a magnetic field or a spin current. Depending on the relative orientation of the two FM layers, the device exhibits two resistance states: “high” (when the two layers are antiparallel to each other) or “low” (when the two layers show parallel orientation of their magnetization). These two states are separated by an energy barrier that is determined by the anisotropy and volume of the FM layers.³⁰ As mentioned in Sec. II, thermal agitation in nanomagnets brings about a distribution of switching fields. A similar effect occurs when these nanomagnets constitute the free layer of an MTJ. The switching current of a STT-MTJ nanopillar also has a distribution due to thermal agitation. The switching probability between the two resistance states depends on the current amplitude and pulse width. Both parameters can be adjusted so that the switching probability of a given MTJ is close to 0.5. In this way, these switching events are the source of true random numbers.^{4,31–33} The main challenge of this approach is the Joule heating power dissipation, which is not negligible and hinders large scale integration of these types of devices. As will be described in detail in Sec. V, the energy efficiency challenge can be tackled by the development of voltage-controlled (i.e., magnetoelectric) MRAMs, where voltage could be used (instead of current) to tailor the anisotropy of the free layer and the magnetic easy axis direction. Implementation of voltage-controlled MRAMs requires precise control of the thickness and microstructure of the magnetic free layer so that its properties can be sensitive to an applied electric field. Another challenge is that the STT-MTJ share the same access path for the read and write operations, thereby causing interference problems and some lack of reliability. This has been overcome using the spin-orbit torque (SOT) effect, instead of STT, which utilizes three terminals instead of two (read/write paths are thus separated).³⁴ In this case, the switching between parallel and antiparallel states is induced by

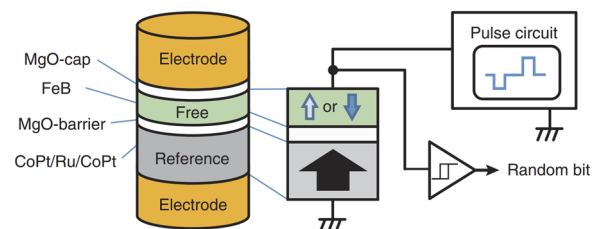


FIG. 6. Schematic diagram of STT-MRAM “spin dice.” Current pulses are injected into a MTJ with perpendicular anisotropy to switch the magnetization in the free layer by spin-transfer-torque (STT).²⁸ Highly reliable random bits can be obtained by comparing resistance values of an array of MTJs comprised in the STT-MRAM. This is sometimes referred to as “differential concept.”³⁴ Reproduced with permission from Fukushima *et al.*, Appl. Phys. Express 7, 083001 (2014). Copyright 2014, The Japan Society of Applied Physics.

an in-plane current that flows along a heavy metal (Pt, Ta, W, and Ir) grown underneath the free layer.^{35,36} In spite of a better robustness, energy loss due to heating effects continues to be a challenge in SOT-RAM true-RNGs.

Randomness in the trajectories of skyrmions (Fig. 4) can also be used to generate random numbers or random sequences. A particular design combined the stochastic dynamics of synthetic AFM skyrmions, driven by spin-polarized currents, with the racetrack memory concept using a topologically bifurcated path with one input branch and two output branches.³⁷ The authors demonstrated that under the steady action of current, skyrmions starting from a continuous nucleation in the input branch were stochastically divided into the two output branches of the device.

B. Exploiting magnetic randomness for physical unclonable functions (data security)

Traditionally, protection of confidential information has relied on the use of passwords generated either by the user or by encryption software. This type of protection is often vulnerable to cyberattacks (phishing, malware, ransomware, and eavesdropping). To minimize security breaches, a new concept was proposed in 2002 when the utilization of the so-called “physical unclonable functions” (PUFs) was first suggested as a hardware alternative to conventional algorithmic “passwords” or encryption procedures.³⁸ A PUF is defined as a collection of robust, singular, unclonable, and unpredictable physical properties of a device, which make it unique (i.e., “device fingerprint”).^{39,40} Such properties can be the result of non-controllable manufacturing imperfections or can originate from stochastic physical phenomena that occur during device operation. These features can be used to generate a series of queries and device responses technically called “challenge-response pairs” (CRPs). Authentication is based on the physical verification of these CRPs. There are many variables that can be used to generate PUFs: local variations of the capacitance across a film containing random assemblies of dielectric particles (“coating PUF”), stochastic switching of superparamagnetic MRAMs with time, and variations of the magnetoresistance state (high/low) in the memory units of STT-MRAMs. Some recent PUF schemes have even taken advantage of carbon nanotubes⁴¹ or plasmonic particles and quantum materials.⁴² PUFs can be implemented with small hardware investment, and they are more energy efficient than tamper-proof security packages existing in the market.

First magnetic PUF designs date back to 1994.⁴³ They were engineered to make unique magnetic swipe cards, such as credit and identity cards, by blending FM particles with random sizes and shapes on a receptor layer. The PUF principle was thus based on the manufacturing variability. More sophisticated magnetic PUFs include an MTJ operating using the toggle principle (where switching is induced by applied magnetic fields⁴⁴ or the STT-MRAMs).⁴⁵ Toggle-MRAM-PUFs take advantage of geometric variations between different MTJ cells, which are used as a digital signature of the device.⁴⁴ Usually, the free layer is affected by thermal agitation. In the case of superparamagnetic MRAM-PUFs, random switching occurs with time in each cell (Sec. II). The working principle of STT-MRAM PUFs is similar to the one described in Sec. IV A for true-RNGs. However, to establish the set of CRPs, an array of

STT-MRAM cells (typically in crossbar geometry) is needed and each MTJ is set to be in a random configuration of high and low resistance states when a critical switching current is applied.^{33,46–50}

Generally speaking, PUF architectures utilizing non-volatile memories are quite new, mostly developed during the last five years. These include, for example, PUFs based on resistive switching materials (RE-RAM PUFs), phase change materials (PCM-PUFs), ferroelectric oxides (FE-RAM PUFs), toggle magnetoresistance (MRAM PUFs), or STT-MRAM PUFs. The advantages and disadvantages of each type of these data security primitives depend on the properties of the constituent materials and the involved switching mechanisms. STT-RAM PUFs are among the most energy efficient (with 10^{-2} pJ/bit), orders of magnitude more efficient than PCM-PUFs (10 pJ/bit), RE-RAM PUFs, or toggle-MRAM PUFs (10^{-1} pJ/bit). Access speed in STT-RAM PUFs (1–10 ns) is also faster than in FE-RAM PUFs (10–100 ns) or flash PUFs ($>10^3$ ns) and comparable to RE-RAM PUFs or toggle MRAM-PUFs.^{39,40,51–59} Thus, magnetic materials exhibiting stochastic transitions can indeed offer unique opportunities in the exciting field of data security.

C. Exploiting magnetic randomness for logics and probabilistic computing

Probabilistic computing is emerging as an intermediate computation paradigm that lies between classical digital computing and quantum computing. At present, quantum computing suffers from some important challenges, such as low-temperature operation and the limited number of many-body interactions that can be implemented. These challenges can be tackled to some extent through probabilistic computing. The basic computation units are the probabilistic p-bits, which are classical entities spontaneously fluctuating in time between “1” and “0” states.^{1,5,34,60} The full potential of p-bits can be realized only when the probability of occurrence of the two possible states can be modulated by an external input.³⁴ Figure 7 shows a schematic comparison between the large energy barrier in the MTJ of a conventional MRAM memory (which would lead to retention times of the order of years) and that of a p-bit based using MTJs with a thinner free layer (leading to retention times of the order of ms).⁵

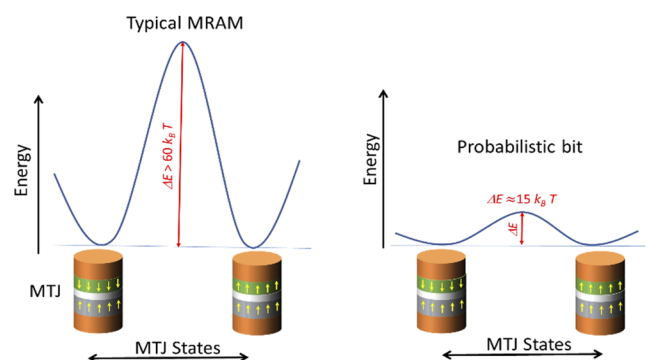


FIG. 7. Illustration of the energy profiles between the parallel and antiparallel states of the free and pinned magnetization orientations in (a) a MTJ for typical MRAM technology (with a large energy barrier) and (b) a probabilistic bit (with much lower energy barrier and retention times in the order of ms). Adapted from Borders *et al.*, *Nature* **573**, 390 (2019). Copyright 2019, Nature Publishing Group.

The energy barrier of the p-bit can be tuned by adjusting the thickness, saturation magnetization, and effective magnetic anisotropy of the free layer in the MTJs. The occurrence of dipolar interactions between the free and pinned layers can lead to not completely random parallel and antiparallel (i.e., non-fully isotropic) configurations, resulting in some probabilities for each of the two states that can be modulated to values different than 0.5.⁶⁰ In STT-MRAMs, such switching probability can be tuned by proper adjustment of the spin-torque currents. In some other cases, the anisotropy of the free layer can be controlled with voltage (by magnetoelectric effects). This offers a wide range of opportunities to use magnetic materials for the implementation of p-bits. In particular, different types of operations (e.g., factorization, invertible logic, Bayesian inference, and combinatorial optimization) can be performed using matrices of correlated MTJ-based p-bit networks that can be read by, e.g., precharge sense amplifiers.^{61,62}

Similarly, by tailoring the design of stochastic nanomagnets (e.g., tuning the effective magnetic anisotropy of $\text{Co}_{60}\text{Fe}_{20}\text{B}_{20}$ circular disks or combining pairs of coupled nanomagnets with in-plane and perpendicular-to-plane anisotropies), the use of probabilistic computing for spin logic operations has been proposed and, to some extent, experimentally demonstrated.^{63–66}

Within the field of stochastic computing, a promising route using skyrmions is the ability to process random bit-streams, instead of individual bits. A bit-stream formed by N bits with “1” or “0” is characterized by the stochastic number p , which is the probability of observing a “1” in the stream. In this sense, a perfect control of individual skyrmions is not critical, and the system would be highly tolerant to soft errors: a collapse of a single skyrmion would not modify significantly the overall p value.^{67,68} When two bit-streams are computed in an AND logic gate (as example), the p value for the output bit-stream is the multiplication of the “ p ” values of the input bit-streams. The use of skyrmions allows for very energy efficient and fast processing, thus being promising candidates for massive parallel computing.⁶⁹ However, to ensure this multiplication property, it is necessary that the input bit-streams are uncorrelated. The thermal-driven randomness in the skyrmion movement has been proposed as the mechanism for reshuffling one bit-stream, before entering the computation gate, in order to avoid the undesired correlations while maintaining the p value.⁶⁸ In Fig. 8, we show a very recent experimental validation of the skyrmionic reshuffling using a continuous single layer stack of $\text{Ta}(5)/\text{Co}_{20}\text{Fe}_{60}\text{B}_{20}(1)/\text{Ta}(0.08)/\text{MgO}(2)/\text{Ta}(5)$ (in parentheses, the thickness of the layers in nm).¹² This reshuffling is an off-chip system, although recent developments on in-chip creation, manipulation, and detection of skyrmions⁷⁰ point to the in-chip integration of skyrmionic systems for stochastic computing.

Another possibility for taking advantage of randomness in skyrmion movement is to consider the interaction with specially designed defects. Recently, by considering this interaction, we have shown that, due to thermal diffusion, the probability that a skyrmion avoids the defect or is being trapped in it can change continuously from 0 to 1 by varying the position where the skyrmion is generated, as shown in Fig. 9.²³ Moreover, we also calculated the probability of survival of a skyrmion along a nanotrack, which depends on the driving current and the interaction with the borders of the track. This, together with evaluation of thermal collapse,⁷¹ opens the path

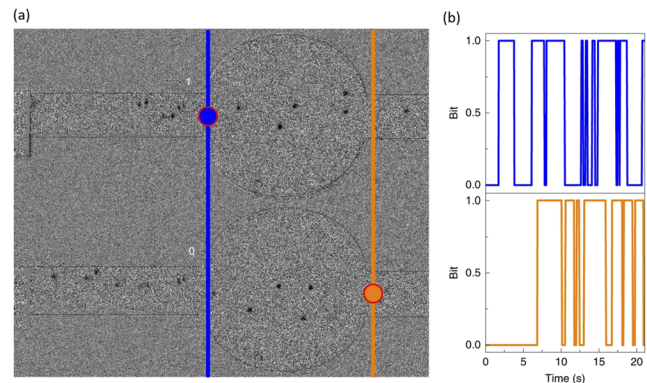


FIG. 8. Reshuffler operation with skyrmion nucleation by a direct current. (a) The input signal is constructed as a time frame in which the skyrmion crosses the blue threshold line. The output is produced on crossing the orange line. (b) The corresponding input signal is depicted in blue (top), and the resulting output signal is depicted in orange (bottom). The radius of the reshuffling chamber is $40\ \mu\text{m}$. The Pearson correlation factor between the input and the output was evaluated as 0.11 ± 0.14 . Reproduced with permission from Zázvorka *et al.*, Nat. Nanotechnol. **14**, 658 (2019). Copyright 2019, Nature Publishing Group.

of using finite nanotracks as probabilistic selectors of skyrmionic bits or bit-streams, as well as for designing stochastic logic gates.

Thus, defects, either engineered or naturally occurring, can have strong interaction with the skyrmions. Recent works studied the dynamics of skyrmions considering random distribution of defects⁷² or randomly distributed granularity.⁷³ Moreover, the dynamics of skyrmions (or other skyrmionic-like structures) in the presence of defects is highly non-linear, which yields the possibility of having critical points (attractors, repeller, and/or saddle points) depending on the input parameters.⁷⁴ This could result in interesting chaotic scenarios.⁷⁵ These systems are at an early stage of their development but could be also envisaged to randomize or shuffle information.

D. Exploiting magnetic randomness for neuromorphic computing

Neuromorphic computing imitates the physical structure of a human brain to perform computational operations. The possible utilization of magnetic randomness for neuromorphic computing applications is still in its infancy.^{30,36,76–80} Yet, stochastic effects are of primary importance in artificial neural networks that are intended to mimic the brain capability to do “pattern recognition” (i.e., object identification by resemblance). It has been proposed that arrays of interconnected magnetic nanowires could trigger further developments in the field of neuromorphic computing.⁸¹ Artificial synapses should possess sufficiently high fault tolerance in order to be able to identify a given object even if there are some errors or differences between the input signal as the pre-recorded pattern (similar to how the brain works).

In recent years, there is growing evidence from the neurologists’ community that the brain performs probabilistic computation based on partially random operations of neurons, synapses, and dendrites. This effect should be emulated in artificial intelligence systems,

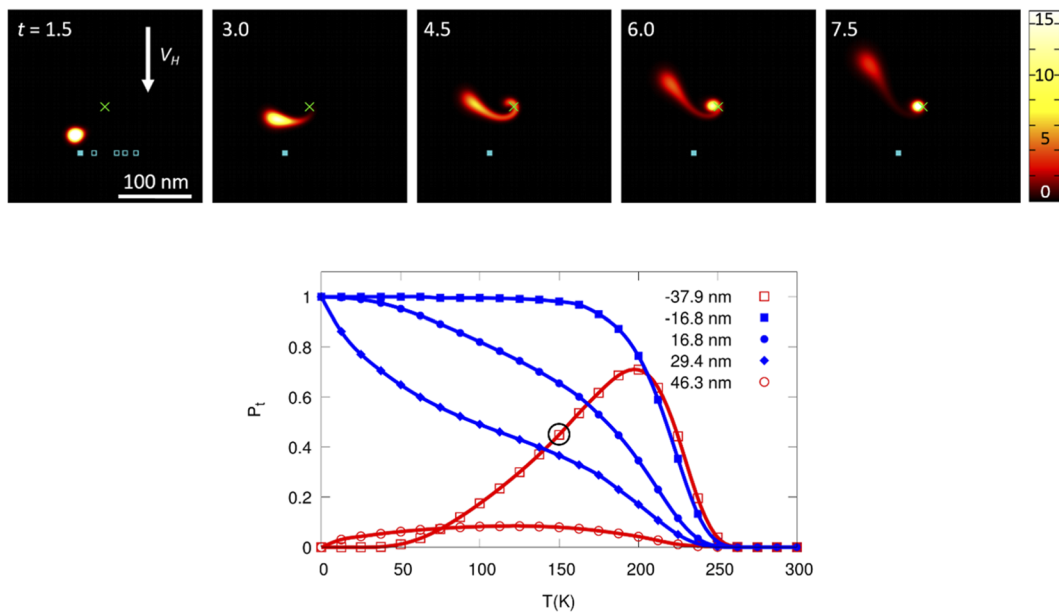


FIG. 9. Snapshots of the probability density (color bar in units of 10^{-3} nm^{-2}) of the presence of a skyrmion as time runs (from left to right, time t in ns). v_H is proportional to the driving spin-current density. This probability can be tuned from 0 to 1 by changing the initial position of the skyrmion and the temperature (bottom). The circle corresponds to the snapshots shown. The two lobes in the last snapshot show clearly that there is a probability (around 0.45 in this case) of being trapped and a probability of escaping (around 0.55). Reproduced with permission from Castell-Queralt *et al.*, Phys. Rev. B **101**, 140404(R) (2020). Copyright 2020, American Physical Society.

particularly for deep learning approaches. The field of magnetoelectricity (voltage control of magnetism) has brought some compelling results into this direction.^{30,79} It has been theoretically proposed that, by using voltage to manipulate the relative orientation of the pinned and free layers in MTJs, such structures can lead to low-power spiking neurons. Magnetoelectric neurons would be encoded through the control of externally applied voltage signals in each individual MTJ.³⁰ The idea is that by applying appropriately shaped voltage pulses, the MTJs can be switched in a probabilistic (rather than fully stochastic) manner. In this way, a probabilistic output stream is generated with a probability that depends on the magnitude of the input stimuli.⁷⁶

The well-known spike timing-dependent plasticity behavior has also been accomplished recently by means of magneto-ionics.⁸⁰ This refers to a particular class of magnetoelectric actuation in which an applied voltage triggers the motion of ions from (or toward) a target magnetic material, depending on the voltage polarity, in order to modify its magnetic properties in a non-volatile (permanent) manner. So far, spike timing-dependent plasticity and other neuromorphic features have been studied in detail in Co/GdO_x bilayers, where GdO_x is an ionic conductor able to provide O²⁻ ions to Co (to reduce its magnetization, emulating forgetting processes, or synaptic depression) or to remove O²⁻ ions from CoO (to increase the magnetization, emulating learning processes, or synaptic potentiation). Non-linear voltage-driven magnetization (M) vs time potentiation/depression curves have been observed in a number of other electrolyte-gated magnetoelectric materials.^{82,83} As an example, Fig. 10(b) shows potentiation–depression magnetic transitions that we measured in mesoporous FeO_x patterned

disks under application of negative and positive voltage long-term pulses.⁸⁴ While there is a general trend for M to always increase (or decrease) for negative (or positive) voltages, respectively, differences in the exact M values among dots (and samples) were also encountered. Namely, due to microstructural differences among the patterned dots, the exact O²⁻ ion diffusion channels generated in different dots were different. Consequently, stochastic magneto-ionic responses were observed. Further randomness can be induced by interconnecting the dots in several paths and applying different voltage pulses in each of the electrical contacts [Fig. 10(c)].

A further development toward neuromorphic computing using magnetic materials is displayed in Fig. 10(d).^{85,86} The basic structure consists of an elongated ferromagnet/heavy metal heterostructure able to stabilize domain walls, which can be moved with the electric current using a three-terminal device (spin-Hall effect). The FM layer in contact with the heavy metal is actually the free layer of a MTJ where multi-level resistive states can be generated through the motion of the domain wall in the free layer. That is, depending on the position of the domain wall, the fraction of the free layer parallel or antiparallel to the pinned layer varies in an analog manner, as required for neuromorphic computing. Simulations on the operation principle of this device suggest that it has the potential to achieve energy consumption as low as 2 pJ per synaptic event, which is comparable to the energy consumption in biological synapses.

Skyrmionic systems have also been proposed for neuromorphic computing.⁸⁷ Again, the tunable current-driven dynamics of skyrmions allows designing systems mimicking the biological neurons, where “skyrmionic synapses” can reproduce the synaptic plasticity and a gradient of perpendicular magnetic anisotropy along

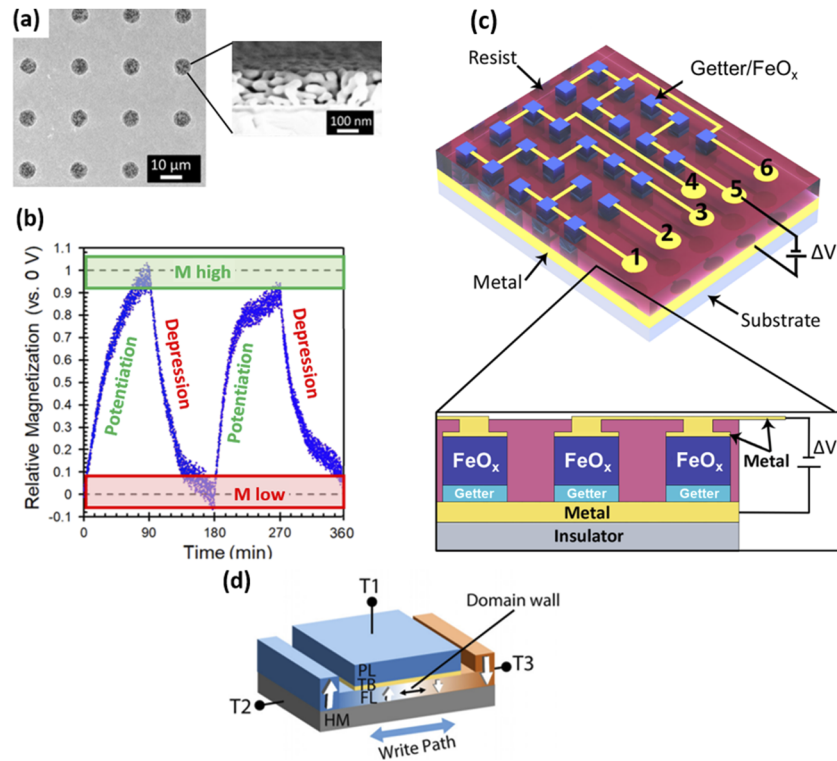


FIG. 10. (a) Scanning electron microscopy image of an array of magnetoelectrically actuated mesoporous FeO_x disks.⁸⁴ (b) Variation of the normalized magnetization with time for FeO_x during two consecutive cycles, first applying $\Delta V = -10$ V (to induce synaptic potentiation) and then $\Delta V = +10$ V (to induce synaptic depression). (c) A solid-state magnetoelectric device that consists of an ordered array of micro-/nano-scale FeO_x interconnected dots, each of them in direct contact with an oxygen getter/donor layer (e.g., Gd, which will become GdO_x upon voltage application). The dots can be electrically connected in a combinatorial fashion, i.e., using different paths, therefore, forming a number of possible circuits. (d) Design of a device able to encode multilevel resistive states through the position of the domain wall in the FM free layer due to the passage of a charge current of appropriate magnitude between terminals T2 and T3. The device state can be “read” between terminals T1 and T3 using the tunneling junction. Note that PL, TB, FL, and HM denote the pinned layer, tunnel barrier, free layer, and heavy metal layer, respectively. Reproduced from Roy *et al.*, J. Appl. Phys. **123**, 210901 (2018) with the permission of AIP Publishing.

a track can be tuned to simulate the leaky-integrate-fire function of a neuron.^{88,89} Experimental versions of such artificial synapses have been built using skyrmions on $[\text{Pt} (3 \text{ nm})/\text{Gd}_{24}\text{Fe}_{66.6}\text{Co}_{9.4} (9 \text{ nm})/\text{MgO} (1 \text{ nm})]_{20}$ ferrimagnetic multilayer stacks, while simulations showed an 89% accuracy in pattern recognition using all-electric skyrmionic artificial synapses.⁸⁷

V. FUTURE OUTLOOK

The utilization of random phenomena in magnetic materials offers formidable challenges for future implementation of innovative technologies, such as new data security primitives, probabilistic logics (with prospects toward quantum computing), or artificial neural networks. Some of the described materials and proposed layouts are compatible with CMOS architectures, and many of them can be readily developed at the chip level (e.g., crossbar arrays for STT-RAMs, arrays of nanomagnets for stochastic computing and logics, and room-temperature skyrmions). However, the current state of the art in these fields faces several challenges, such as (i) need for improved control of randomness for probabilistic computing (beyond the approaches described in Sec. III), (ii) need for

enhanced energy efficiency (bearing in mind that 20% of the global energy will be spent in information technologies by 2030⁹⁰), (iii) further compatibility with existing CMOS technologies, (iv) enhanced endurance (cyclability) to increase the lifetime of devices, or (v) faster operation speed (ideally toward sub- μs), among others.

Many of newly proposed stochastic magnetic devices are based on STT-MRAMs. The endurance of STT-MRAM PUF systems is sometimes compromised by the dielectric breakdown of the insulating barrier layer resulting from repeated applied electric pulses, which cause stress and degradation. Similar to true-RNGs, the use of (SOT)-PUFs has been recently suggested as an alternative to overcome this limitation.^{35,91} Interestingly, new strategies are being proposed to enhance tamper resistance (ability to detect a cyberattack) by means of new STT- and SOT-MRAM PUF architectures,⁴⁷ thereby surpassing the functionalities of other types of non-magnetic PUFs. Recently, STT magnetic tunnel junction architectures have also been proposed for their use as spintronic nano-oscillators, which allow for new neuromorphic functionalities at high frequencies, such as pattern recognition.^{92,93} However, this technology (STT-MRAMs or SOT-MRAMs) utilizes spin-polarized currents, which still involves a significant power dissipation in the

form of Joule heating effect. In recent years, voltage-driven switching of nanomagnets has gained interest as an alternative to STT effects. By using voltage instead of current to control the magnetic properties of materials, important energy savings are expected. Switching energies as low as 10^{-6} pJ/bit have been theoretically predicted for optimized strain-mediated magnetoelectric materials.⁵⁵ So far, switching energies of the order of 10^{-3} pJ/bit have been experimentally reported in both multiferroic heterostructures and magneto-ionic systems.^{55,94} Yet, the implementation of stochastic devices based on the use of magnetoelectric materials is still at the early stages.^{29,95,96} Aspects such as clamping effects with the substrate (in the case of strain-mediated ferroelectric/magnetostrictive bilayers), reduction of the needed threshold voltages to induce the desired effects, or full reversibility upon successive application of repeated voltage pulses still require further optimization and new materials engineering. In turn, magneto-ionic materials based on O^{2-} ion migration often suffer from limited cyclability (endurance) (sometimes not exceeding 100 cycles), and the rates at which ions diffuse can be rather slow (\sim seconds or, in some cases, ms). These switching rates are too slow for memory applications but can still be convenient for neuromorphic applications. Progress at the material level has been accomplished by replacing materials based on O^{2-} ion motion by others governed by different ion species, such as N^{3-} or H^{+} , which have been shown to diffuse faster.^{97,98} Remarkably, it has been proposed that the proton-based magneto-ionic approach can also induce new functionalities, such as Dzyaloshinskii–Moriya interactions.⁹⁹ Further materials engineering could boost magnetonics. In particular, control of structural defects [e.g., vacancies] and grain boundaries (which often act as fast diffusion paths¹⁰⁰) are suitable strategies to improve the performance of these types of materials. In this direction, the creation of vertically aligned nanostructures (VANs) with magneto-ionic characteristics can be proposed as an alternative to continuous thin films or planar patterned dots.^{101,102}

Concerning skyrmions, although they can be moved with high efficiency (with currents of the order of 10^6 Am⁻², i.e., several orders of magnitude lower than the currents needed to move domain walls) and progress in the control of individual skyrmions has been made, there is still a large room for further adjustment of their randomness.¹⁰³ Issues such as the interaction with defects; thermal influence on realistic devices; and faster and better reproducible ways of generating, moving, and detecting skyrmions need deeper investigations. In addition, other skyrmionic-like structures can also be studied for randomized systems (e.g., AFM skyrmions and antiskyrmions).

Concerning operation speeds, true-RNGs and PUFs based on STT-MRAMs are already very fast (of the order of ns). Conversely, faster rates are needed in magneto-ionic materials. In skyrmions, velocities larger than 10 m/s have been reported,¹⁰⁴ but the speed is largely affected by the granularity of the track or the presence of defects. Probabilistic control of the randomness of skyrmion Brownian motion via periodic pinning sites in their propagation tracks faces the challenge of the concomitant reduction in the working speed of the resulting logic device. Hence, further research is needed to optimize this interplay of effects and to implement stochastic/probabilistic devices operating at competitive speeds.

Finally, stochastic effects have also been reported, very recently, in artificial spin networks, a particular type of magnetic

metamaterial in which a large number of nanoscale magnetic elements are coupled together to render controllable random responses (i.e., tunable probability distributions) based on stochasticity in magnetic domain wall motion (domain wall sinks) at the nanoscale.¹⁰⁵ It has been claimed that such types of materials can be exploited to perform complex computational tasks, beyond conventional Von Neumann computing paradigms.

ACKNOWLEDGMENTS

This project received funding from the European Research Council (MAGIC-SWITCH 2019-Proof of Concept Grant No. 875018), the *Agencia Estatal de Investigación* of the Spanish Government (Grant Nos. MAT2017-86357-C3-1-R and PID2019-104670GB-I00 and associated FEDER), and the Generalitat de Catalunya (Grant Nos. 2017-SGR-292 and 2017-SGR-105). We would like to thank Dr. C. Navarro-Senent, Dr. A. Nicolenco, and J. Castell-Queralt for assisting us with the preparation of some layouts for the figures.

DATA AVAILABILITY

The data that support the findings of this study are available from the corresponding authors upon reasonable request.

REFERENCES

- K. Y. Camsari, P. Debashis, V. Ostwal, A. Z. Pervaiz, T. Shen, Z. Chen, S. Datta, and J. Appenzeller, *Proc. IEEE* **108**, 1322–1337 (2020).
- L. Zhao, Z. Wang, X. Zhang, X. Liang, J. Xia, K. Wu, H.-A. Zhou, Y. Dong, G. Yu, K. L. Wang, X. Liu, Y. Zhou, and W. Jiang, *Phys. Rev. Lett.* **125**, 027206 (2020).
- M.-Y. Im, P. Fischer, K. Yamada, T. Sato, S. Kasai, Y. Nakatani, and T. Ono, *Nat. Commun.* **3**, 983 (2012).
- R. Carboni and D. Ielmini, “Applications of resistive switching memory as hardware security primitive,” in *Applications of Emerging Memory Technology*, Springer Series in Advanced Microelectronics Vol. 63, edited by M. Suri (Springer, Singapore, 2020).
- W. A. Borders, A. Z. Pervaiz, S. Fukami, K. Y. Camsari, H. Ohno, and S. Datta, *Nature* **573**, 390 (2019).
- A. Ekert and R. Jozsa, *Rev. Mod. Phys.* **68**, 733 (1996).
- C. A. Ross, S. Haratani, F. J. Castaño, Y. Hao, M. Hwang, M. Shima, J. Y. Cheng, B. Vögeli, M. Farhoud, M. Walsh, and H. I. Smith, *J. Appl. Phys.* **91**, 6848 (2002).
- C. Safranski, J. Kaiser, P. Trouilloud, P. Hashemi, G. Hu, and J. Z. Sun, *Nano Lett.* **21**, 2040 (2021).
- G. Salazar-Alvarez, J. J. Kavich, J. Sort, A. Mugarza, S. Stepanow, A. Potenza, H. Marchetto, S. S. Dhesi, V. Baltz, B. Dieny, A. Weber, L. J. Heyderman, J. Nogués, and P. Gambardella, *Appl. Phys. Lett.* **95**, 012510 (2009).
- C. C. H. Lo, E. R. Kinser, and D. C. Jiles, *J. Appl. Phys.* **99**, 08B705 (2006).
- T. J. Hayward, *Sci. Rep.* **5**, 13279 (2015).
- J. Závorka, F. Jakobs, D. Heinze, N. Keil, S. Kromin, S. Jaiswal, K. Litzius, G. Jakob, P. Virnau, D. Pinna, K. Everschor-Sitte, L. Rózsa, A. Donges, U. Nowak, and M. Kläui, *Nat. Nanotechnol.* **14**, 658 (2019).
- T. Nozaki, Y. Jibiki, M. Goto, E. Tamura, T. Nozaki, H. Kubota, A. Fukushima, S. Yuasa, and Y. Suzuki, *Appl. Phys. Lett.* **114**, 012402 (2019).
- G. Finocchio and C. Panagopoulos, in *Magnetic Skyrmions and Their Applications* (Woodhead Publishing, U.K., 2021).
- S. Brück, J. Sort, V. Baltz, S. Suriñach, J. S. Muñoz, B. Dieny, M. D. Baró, and J. Nogués, *Adv. Mater.* **17**, 2978 (2005).
- S. Agramunt-Puig, N. Del-Valle, C. Navau, and A. Sanchez, *Appl. Phys. Lett.* **104**, 012407 (2014).
- V. Cambel and G. Karapetrov, *Phys. Rev. B* **84**, 014424 (2011).
- J. Brandão, R. L. Novak, H. Lozano, P. R. Soledade, A. Mello, F. Garcia, and L. C. Sampaio, *J. Appl. Phys.* **116**, 193902 (2014).

- ¹⁹R. K. Dumas, T. Gredig, C. P. Li, I. K. Schuller, and K. Liu, *Phys. Rev. B* **80**, 014416 (2009).
- ²⁰R. K. Dumas, D. A. Gilbert, N. Eibagi, and K. Liu, *Phys. Rev. B* **83**, 060415(R) (2011).
- ²¹A. Gómez, F. Cebollada, F. J. Palomares, N. Sanchez, E. M. Gonzalez, J. M. Gonzalez, and J. L. Vicent, *Appl. Phys. Lett.* **104**, 102406 (2014).
- ²²D. A. Gilbert, B. B. Maranville, A. L. Balk, B. J. Kirby, P. Fischer, D. T. Pierce, J. Unguris, J. A. Borchers, and K. Liu, *Nat. Commun.* **6**, 8462 (2015).
- ²³J. Castell-Queralt, L. González-Gómez, N. Del-Valle, and C. Navau, *Phys. Rev. B* **101**, 140404(R) (2020).
- ²⁴G. Yu, P. Upadhyaya, Q. Shao, H. Wu, G. Yin, X. Li, C. He, W. Jiang, X. Han, P. K. Amiri, and K. L. Wang, *Nano Lett.* **17**, 261 (2017).
- ²⁵W. Jiang, P. Upadhyaya, W. Zhang, G. Yu, M. B. Jungfleisch, F. Y. Fradin, J. E. Pearson, Y. Tserkovnyak, K. L. Wang, O. Heinonen, S. G. E. te Velthuis, and A. Hoffmann, *Science* **349**, 283 (2015).
- ²⁶S. Woo, K. Litzius, B. Krüger, M.-Y. Im, L. Caretta, K. Richter, M. Mann, A. Krone, R. M. Reeve, M. Weigand, P. Agrawal, I. Lemesch, M.-A. Mawass, P. Fischer, M. Kläui, and G. S. D. Beach, *Nat. Mater.* **15**, 501 (2016).
- ²⁷W. Jiang, G. Chen, K. Liu, J. Zhang, S. G. E. te Velthuis, and A. Hoffmann, *Phys. Rep.* **704**, 1 (2017).
- ²⁸A. Fukushima, T. Seki, K. Yakushiji, H. Kubota, H. Imamura, S. Yuasa, and K. Ando, *Appl. Phys. Express* **7**, 083001 (2014).
- ²⁹A. Fukushima, T. Yamamoto, T. Nozaki, K. Yakushiji, H. Kubota, and S. Yuasa, *APL Mater.* **9**, 030905 (2021).
- ³⁰K. Yang and A. Sengupta, *Appl. Phys. Lett.* **116**, 043701 (2020).
- ³¹M. N. I. Khan, C. Y. Cheng, S. H. Lin, A. Ash-Saki, and S. Ghosh, *J. Low Power Electron. Appl.* **11**, 5 (2021).
- ³²D. Vodenicarevic, N. Locatelli, A. Mizrahi, J. S. Friedman, A. F. Vincent, M. Romera, A. Fukushima, K. Yakushiji, H. Kubota, S. Yuasa, S. Tiwari, J. Grollier, and D. Querlioz, *Phys. Rev. Appl.* **8**, 054045 (2017).
- ³³B. Perach and S. Kvatinsky, *IEEE Trans. Very Large Scale Integr. VLSI Syst.* **27**, 2473 (2019).
- ³⁴P. Debashis, R. Faria, K. Y. Camsari, S. Datta, and Z. Chen, *Phys. Rev. B* **101**, 094405 (2020).
- ³⁵G. Finocchio, T. Moriyama, R. De Rose, G. Siracusano, M. Lanuzza, V. Puliafito, S. Chiappini, F. Crupi, Z. Zeng, T. Ono, and M. Carpentieri, *J. Appl. Phys.* **128**, 033904 (2020).
- ³⁶R. Carboni and D. Ielmini, *Adv. Electron. Mater.* **5**, 1900198 (2019).
- ³⁷I. Medlej, A. Hamadeh, and F. E. H. Hassan, *Physica B* **579**, 411900 (2020).
- ³⁸R. Pappu, B. Recht, J. Taylor, and N. Gershenfeld, *Science* **297**, 2026 (2002).
- ³⁹Y. Gao, S. F. Al-Sarawi, and D. Abbott, *Nat. Electron.* **3**, 81 (2020).
- ⁴⁰T. McGrath, I. E. Bagci, Z. M. Wang, U. Roedig, and R. J. Young, *Appl. Phys. Rev.* **6**, 011303 (2019).
- ⁴¹Z. Hu, J. M. M. L. Comeras, H. Park, J. Tang, A. Afzali, G. S. Tulevski, J. B. Hannon, M. Liehr, and S.-J. Han, *Nat. Nanotechnol.* **11**, 559 (2016).
- ⁴²A. F. Smith, P. Patton, and S. E. Skrabalak, *Adv. Funct. Mater.* **26**, 1315 (2016).
- ⁴³R. S. Indeck and M. W. Muller, "Method and apparatus for fingerprinting magnetics media" U.S. patent US5365586A (1994).
- ⁴⁴J. Das, K. Scott, and S. Bhanja, *ACM J. Emerg. Technol. Comput. Syst.* **13**, 1 (2016).
- ⁴⁵C.-H. Chang, Y. Zheng, and L. Zhang, *IEEE Circuits Syst. Mag.* **17**, 32 (2017).
- ⁴⁶T. Marukame, T. Tanamoto, and Y. Mitani, *IEEE Trans. Magn.* **50**, 3402004 (2014).
- ⁴⁷S. Ben Dodo, R. Bishnoi, S. Mohanachandran Nair, and M. B. Tahoori, *IEEE Trans. Very Large Scale Integr. VLSI Syst.* **27**, 2511 (2019).
- ⁴⁸E. I. Vatajelu, G. D. Natale, and P. Prinetto, in *IEEE 34th VLSI Test Symposium (VTS)* (IEEE, 2016), p. 1.
- ⁴⁹L. Zhang, X. Fong, C. Chang, Z. H. Kong, and K. Roy, in *2014 IEEE International Symposium on Circuits and Systems (ISCAS)* (IEEE, 2014), p. 2169.
- ⁵⁰S. Takaya, T. Tanamoto, H. Noguchi, K. Ikegami, K. Abe, and S. Fujita, *Jpn. J. Appl. Phys., Part 1* **56**, 04CN07 (2017).
- ⁵¹Y. Gao, D. C. Ranasinghe, S. F. Al-Sarawi, O. Kavehei, and D. Abbott, *IEEE Access* **4**, 61 (2016).
- ⁵²J.-M. Hu, Z. Li, L.-Q. Chen, and C.-W. Nan, *Adv. Mater.* **24**, 2869 (2012).
- ⁵³H. Cai, W. Kang, Y. Wang, L. Alves De Barros Naviner, J. Yang, and W. Zhao, *Appl. Sci.* **7**, 929 (2017).
- ⁵⁴S. Manipatrundi, D. E. Nikonov, C.-C. Lin, T. A. Gosavi, H. Liu, B. Prasad, Y.-L. Huang, E. Bonturim, R. Ramesh, and I. A. Young, *Nature* **565**, 35 (2019).
- ⁵⁵J.-M. Hu and C.-W. Nan, *APL Mater.* **7**, 080905 (2019).
- ⁵⁶K. L. Wang, H. Lee, and P. Khalili Amiri, *IEEE Trans. Nanotechnol.* **14**, 992 (2015).
- ⁵⁷A. D. Kent and D. C. Worledge, *Nat. Nanotechnol.* **10**, 187 (2015).
- ⁵⁸L. Zhang, X. Fong, C.-H. Chang, Z. H. Kong, and K. Roy, in *2014 IEEE 6th International Memory Workshop (IMW)* (IEEE, 2014), p. 1.
- ⁵⁹E. I. Vatajelu, G. D. Natale, M. Barbareschi, L. Torres, M. Indaco, and P. Prinetto, *ACM J. Emerg. Technol. Comput. Syst.* **13**, 5 (2016).
- ⁶⁰Y. Cao, G. Xing, H. Lin, N. Zhang, H. Zheng, and K. Wang, *iScience* **23**, 101614 (2020).
- ⁶¹M. W. Daniels, A. Madhavan, P. Talatchian, A. Mizrahi, and M. D. Stiles, *Phys. Rev. Appl.* **13**, 034016 (2020).
- ⁶²K. Y. Camsari, R. Faria, B. M. Sutton, and S. Datta, *Phys. Rev. X* **7**, 031014 (2017).
- ⁶³P. Debashis, R. Faria, K. Y. Camsari, and Z. Chen, *IEEE Magn. Lett.* **9**, 4305205 (2018).
- ⁶⁴K. Y. Camsari, B. M. Sutton, and S. Datta, *Appl. Phys. Rev.* **6**, 011305 (2019).
- ⁶⁵R. Faria, K. Y. Camsari, and S. Datta, *IEEE Magn. Lett.* **8**, 4105305 (2017).
- ⁶⁶P. Debashis and Z. Chen, *Sci. Rep.* **8**, 11405 (2018).
- ⁶⁷S. Li, W. Kang, X. Zhang, T. Nie, Y. Zhou, K. L. Wang, and W. Zhao, *Mater. Horiz.* **8**, 854 (2021).
- ⁶⁸D. Pinna, F. Abreu Araujo, J.-V. Kim, V. Cros, D. Querlioz, P. Bessiere, J. Droulez, and J. Grollier, *Phys. Rev. Appl.* **9**, 064018 (2018).
- ⁶⁹H. Zhang, D. Zhu, W. Kang, Y. Zhang, and W. Zhao, *Phys. Rev. Appl.* **13**, 054049 (2020).
- ⁷⁰Z. Wang, M. Guo, H.-A. Zhou, L. Zhao, T. Xu, R. Tomasello, H. Bai, Y. Dong, S.-G. Je, W. Chao, H.-S. Han, S. Lee, K.-S. Lee, Y. Yao, W. Han, C. Song, H. Wu, M. Carpentieri, G. Finocchio, M.-Y. Im, S.-Z. Lin, and W. Jiang, *Nat. Electron.* **3**, 672–679 (2020).
- ⁷¹A. Derras-Chouk, E. M. Chudnovsky, and D. A. Garanin, *J. Appl. Phys.* **126**, 083901 (2019).
- ⁷²C. Reichhardt and C. J. O. Reichhardt, *Phys. Rev. B* **99**, 104418 (2019).
- ⁷³A. Salimath, A. Abbout, A. Brataas, and A. Manchon, *Phys. Rev. B* **99**, 104416 (2019).
- ⁷⁴L. González-Gómez, J. Castell-Queralt, N. Del-Valle, A. Sanchez, and C. Navau, *Phys. Rev. B* **100**, 054440 (2019).
- ⁷⁵L. Shen, J. Xia, X. Zhang, M. Ezawa, O. A. Tretiakov, X. Liu, G. Zhao, and Y. Zhou, *Phys. Rev. Lett.* **124**, 037202 (2020).
- ⁷⁶A. Sengupta, P. Panda, P. Wijesinghe, Y. Kim, and K. Roy, *Sci. Rep.* **6**, 30039 (2016).
- ⁷⁷G. Srinivasan, A. Sengupta, and K. Roy, *Sci. Rep.* **6**, 29545 (2016).
- ⁷⁸A. Nisar, F. A. Khanday, and B. K. Kaushik, *Nanotechnology* **31**, 504001 (2020).
- ⁷⁹I. Chakraborty, A. Agrawal, A. Jaiswal, G. Srinivasan, and K. Roy, *Philos. Trans. R. Soc. A* **378**, 20190157 (2019).
- ⁸⁰R. Mishra, D. Kumar, and H. Yang, *Phys. Rev. Appl.* **11**, 054065 (2019).
- ⁸¹E. C. Burks, D. A. Gilbert, P. D. Murray, C. Flores, T. E. Felter, S. Charnvanichborikarn, S. O. Kucheyev, J. D. Colvin, G. Yin, and K. Liu, *Nano Lett.* **21**, 716 (2021).
- ⁸²C. Navarro-Senent, A. Quintana, E. Menéndez, E. Pellicer, and J. Sort, *APL Mater.* **7**, 030701 (2019).
- ⁸³S. Robbenolt, E. Menéndez, A. Quintana, A. Gómez, S. Auffret, V. Baltz, E. Pellicer, and J. Sort, *Sci. Rep.* **9**, 10804 (2019).
- ⁸⁴M. Cialone, A. Nicolenco, S. Robbenolt, E. Menéndez, G. Rius, and J. Sort, *Appl. Mater. Interfaces* **8**, 2001143 (2021).
- ⁸⁵A. Sengupta, Z. Al Azim, X. Fong, and K. Roy, *Appl. Phys. Lett.* **106**, 093704 (2015).
- ⁸⁶K. Roy, A. Sengupta, and Y. Shim, *J. Appl. Phys.* **123**, 210901 (2018).
- ⁸⁷K. M. Song, J.-S. Jeong, B. Pan, X. Zhang, J. Xia, S. Cha, T.-E. Park, K. Kim, S. Finizio, J. Raabe, J. Chang, Y. Zhou, W. Zhao, W. Kang, H. Ju, and S. Woo, *Nat. Electron.* **3**, 148 (2020).

- ⁸⁸S. Li, W. Kang, Y. Huang, X. Zhang, Y. Zhou, and W. Zhao, *Nanotechnology* **28**, 31LT01 (2017).
- ⁸⁹X. Chen, W. Kang, D. Zhu, X. Zhang, N. Lei, Y. Zhang, Y. Zhou, and W. Zhao, *Nanoscale* **10**, 6139 (2018).
- ⁹⁰N. Jones, *Nature* **561**, 163 (2018).
- ⁹¹M. Kharbouche-Harrari, R. Alhalabi, J. Postel-Pellerin, R. Wacquez, D. Aboulkassimi, E. Nowak, I. L. Prejebeanu, G. Prenat, and G. D. Pendina, in *2018 Conference on Design of Circuits and Integrated Systems (DCIS)* (IEEE, 2018), p. 1.
- ⁹²K. L. Wang *et al.*, *IEEE Trans. Nanotechnol.* **14**, 992 (2015).
- ⁹³J. Torreon, M. Riou, F. Abreu Araujo, S. Tsunegi, G. Khalsa, D. Querlioz, P. Bortolotti, V. Cros, K. Yakushiji, A. Fukushima, H. Kubota, S. Yuasa, M. D. Stiles, and J. Grollier, *Nature* **547**, 428 (2017).
- ⁹⁴M. Romera, P. Talatchian, S. Tsunegi, F. Abreu Araujo, V. Cros, P. Bortolotti, J. Trastoy, K. Yakushiji, A. Fukushima, H. Kubota, S. Yuasa, M. Ernoult, D. Vodenicarevic, T. Hirtzlin, N. Locatelli, D. Querlioz, and J. Grollier, *Nature* **563**, 230 (2018).
- ⁹⁵A. Lee, D. Wu, and K. L. Wang, *IEEE Magn. Lett.* **10**, 4107604 (2019).
- ⁹⁶H. Lee, C. Grezes, A. Lee, F. Ebrahimi, P. Khalili Amiri, and K. L. Wang, *IEEE Electron Device Lett.* **38**, 281 (2017).
- ⁹⁷A. J. Tan, M. Huang, C. O. Avci, F. Büttner, M. Mann, W. Hu, C. Mazzoli, S. Wilkins, H. L. Tuller, and G. S. D. Beach, *Nat. Mater.* **18**, 35 (2019).
- ⁹⁸J. de Rojas, A. Quintana, A. Lopeandía, J. Salguero, B. Muñoz, F. Ibrahim, M. Chshiev, A. Nicolenco, M. O. Liedke, M. Butterling, A. Wagner, V. Sireus, L. Abad, C. J. Jensen, K. Liu, J. Nogués, J. L. Costa-Krämer, E. Menéndez, and J. Sort, *Nat. Commun.* **11**, 5871 (2020).
- ⁹⁹G. Chen, M. Robertson, M. Hoffmann, C. Ophus, A. L. Fernandes Cauduro, R. Lo Conte, H. Ding, R. Wiesendanger, S. Blügel, A. K. Schmid, and K. Liu, *Phys. Rev. X* **11**, 021015 (2021).
- ¹⁰⁰A. Quintana, E. Menéndez, M. O. Liedke, M. Butterling, A. Wagner, V. Sireus, P. Torruella, S. Estradé, F. Peiró, J. Dendooven, C. Detavernier, P. D. Murray, D. A. Gilbert, K. Liu, E. Pellicer, J. Nogués, and J. Sort, *ACS Nano* **12**, 10291 (2018).
- ¹⁰¹O. J. Lee, S. Misra, H. Wang, and J. L. MacManus-Driscoll, *APL Mater.* **9**, 030904 (2021).
- ¹⁰²A. Nicolenco, M. de h-Óra, C. Yun, J. MacManus-Driscoll, and J. Sort, *APL Mater.* **9**, 020903 (2021).
- ¹⁰³A. Fert, V. Cros, and J. Sampaio, *Nat. Nanotechnol.* **8**, 152 (2013).
- ¹⁰⁴X. Gong, H. Y. Yuan, and X. R. Wang, *Phys. Rev. B* **101**, 064421 (2020).
- ¹⁰⁵D. Sanz-Hernández, M. Massouras, N. Reyren, N. Rougemaille, V. Schänilec, K. Bouzehouane, M. Hehn, B. Canals, D. Querlioz, J. Grollier, F. Montaigne, and D. Lacour, *Adv. Mater.* **33**, 2008135 (2021).